JOURNAL OF MATERIALS SCIENCE 26 (1991) 4116 4122

Thermal stability of ceramic fibre in a CVI-processed SiC matrix composite

W. LIN, J-M. YANG
Department of Materials Science and Engineering, University of California, Los Angeles, CA 90024, USA

The thermal stability of the HPZ fibre in a chemical vapour infiltration (CVI)-processed SiC matrix composite was studied. The mechanical properties and fracture behaviour of the untreated and SiC-coated fibres after thermal exposure at different temperatures and atmospheres were characterized. The results show that, below 1000 °C, the strength degradation is negligible. However, severe degradation occurs at temperatures above 1000 °C due to the evolution of CO, SiO, and other gaseous species. Also, pyrolytic C-coating is needed to tailor the interfacial bond strength in the HPZ/SiC composite.

1. Introduction

The incorporation of continuous fibres into ceramics offers a promising route to the production of tough and reliable ceramic materials. With the growing interest in developing fibre-reinforced ceramic matrix composites for high-temperature structural applications, the demand for small-diameter ceramic fibres with high strength, high stiffness, and temperature capability in excess of 1400 °C is continuously increasing. During the last decade, several ceramic fibres have been developed as reinforcements for ceramic composites. Silicon carbide fibres, such as Nicalon and Tyranno, have been widely used as the reinforcement for glass-ceramics and silicon carbides. Oxide fibre, including FP, Nextel 312, and Nextel 440, have also been commercially available for some time. However, a critical issue for utilization of these fibres is their thermal stability. These fibres are vulnerable to severe property degradation due to decomposition, oxidation crystallization, accelerated grain growth, or a combination of these phenomena during high-temperature processing and service environment [1, 2]. The fibre degradation limits not only the high-temperature performance of composites but also the processing routes available for consolidating the composites.

Chemical vapour infiltration (CVI) is one of the most promising reaction-forming processes for making ceramic matrix composites. This process has several potential advantages including the abilities to manipulate and modify the microstructure of the matrix (stoichiometry, crystal orientation, etc.), to tailor the fibre/matrix interface by using different reagents but the same equipments, and to fabricate complex near-net shape components [3]. More importantly, the processing temperature and pressure of the CVI technique are generally much lower relative to other consolidating processes. Nevertheless, the combination of longer processing time and the presence of free elemental constituents tends to degrade the fibres.

The purpose of this work was to evaluate the thermal stability of the HPZ fibre under a typical CVI processing of SiC matrix composites. The microstructure, mechanical properties, and fracture behaviour of the fibres in the as-processed state and after thermal exposure in simulated CVI processing conditions were studied.

2. Experimental procedure

2.1. Ceramic fibre

HPZ fibre is a new ceramic fibre developed by Dow Corning for plastic and ceramic matrix composites. This fibre is derived from hydridipolysilazane polymer produced by the reaction of trichlorosilane ($HSiCl_3$) with hexamethyldisilazane ($(Me_3Si)_2NH$). The polymer is converted into a fibre form by melt spining. The fibre is then cross-linked by exposing to trichlorosilane and pyrolysed at 1200 °C in an inert atmosphere [4]. The fibres are completely amorphous with a normal density of 2.5 g cm^{-3}. Typical bulk composition of this fibre is 59 wt % Si, 29 wt % N, 10 wt % C, and 2 wt % O.

2.2. Deposition of SiC matrix

The matrix was deposited around the fibre by chemical vapour deposition in a hot-wall reactor. The silicon carbide was deposited by the thermal pyrolysis of methyltrichlorosilane (MTS) at 950 °C for 5 min. Pyrolytic C was coated on to the fibres by the thermal pyrolysis of methane at 950 °C to modify the fibre/matrix interface. Hydrogen was used as the carrier gas.

2.3. Thermal exposure

Isothermal exposure of the fibres under vacuum and an oxidizing atmosphere was conducted. The thermal

0022–2461/91 $03.00 + .12

TABLE I Summary of specimen preparation

Specimen designation	Materials specification
HPZ-A	As-fabricated (with C-1 sizing)
HPZ-B	Coated with pyrolytic carbon
HPZ-C	Coated with SiC
HPZ-D	Coated with pyrolytic carbon and SiC
HPZ-A-1	H.T. in vacuum at 950 °C, 16 h
HPZ-A-2	H.T. in vacuum at 950 °C, 100 h
HPZ-A-3	H.T. in vacuum at 950°C, 360 h
HPZ-A-4	H.T. in vacuum at 950 °C, 650 h
HPZ-A-5	H.T. in H_2 at 950 °C, 2 h
HPZ-A-6	H.T. in air at 1200 °C, 2 h
HPZ-A-7	H.T. in air at 1200 °C, 64 h
HPZ-A-8	H.T. in vacuum at 1200 °C, 2 h
HPZ-A-9	H.T. in vacuum at 1200 °C, 64 h
HPZ-D-1	H.T. in vacuum at 950 °C, 16 h
HPZ-D-2	H.T. in vacuum at 950 °C, 100 h
HPZ-D-3	H.T. in vacuum at 950 °C, 260 h

exposure was designed to simulate the conditions experienced by the fibres during processing and service. The as-fabricated fibre and those coated with pyrolytic C/SiC were exposed to 950 and 1200 °C, respectively. In the case of thermal exposure under vacuum, fibres were sealed in a quartz tube and then put into the furnace for different periods of time. For treatment under the oxidizing atmosphere, fibres were simply exposed in air. Table I lists the thermal treatment evaluated in this study.

2.4. Tensile testing and fracture analysis

Tensile testing was conducted in accordance with the ASTM D-3379-33. Individual fibres were mounted with epoxy cement on "picture frame" holders with gauge length ranging from 25.4–76.2 mm. The test was carried out at room temperature on an Instron testing machine with type A load cell. A crosshead speed of 0.5 mm min^{-1} was used and at least 30 specimens were tested for each condition. Tensile strength was obtained by dividing the maximum load with the average fibre cross-sectional area. The average cross-sectional area of the fibre was measured from the scanning electron micrograph. Young's modulus was determined using a modified method proposed by Langley [5]. The Weibull modulus was also calculated by a least squares fit through the plot of $\ln\ln(1/P_s)$ versus $\ln\sigma$, where P_s is the probability of survival under stress, σ is the fracture strength of the fibre. After testing, the fracture surfaces were examined by a scanning electron microscopy (SEM).

2.5. Structural analysis

X-ray diffraction (XRD) analysis was conducted to study the fibre structure. Fibres (as-fabricated and after thermal exposure) were ground and mixed with Duco-cement for analysis. An X-ray diffractometer with CuK_α radiation was used.

3. Results

3.1. Morphology

The typical surface morphology of the as-fabricated fibre is shown in Fig. 1. The fibre surface is fairly smooth and the cross-section in this fibre is near elliptical in shape. Fig. 2 shows the fracture morphologies of the SiC-coated fibres. It is clear that the coating is uniformly deposited and adheres well to the fibres. The thickness of the silicon carbide coating in this study was about 0.8 μm.

3.2. Mechanical and fracture behaviour

Under tension, the as-fabricated fibre exhibited a linear elastic behaviour until fracture. The average tensile strength and Young's modulus of the as-fabricated fibre with a gauge length of 25.4 mm are 1200 MPa and 188 GPa, respectively. Fig. 3 shows the effect of gauge length on the tensile strength of the as-fabricated HPZ fibre. With increasing gauge length the average tensile strength decreases while Young's modulus remains the same. Fig. 4 shows the plot of $\ln\ln(1/[P(\sigma)])$ versus $\ln\sigma$ of the as-fabricated fibre. A fairly linear relationship was obtained. The Weibull shape parameter, m, was calculated to be 5.4 ± 0.3. The fracture surfaces of as-fabricated fibres under tension are shown in Fig. 5. Surface and internal flaws were observed, and mirror and hackle regions can also be seen in these figures.

Fig. 6 shows the strength distribution of as-fabricated and coated fibres. For those with pyrolytic C coating, the average tensile strength and Young's modulus are 1050 MPa and 180 GPa, respectively.

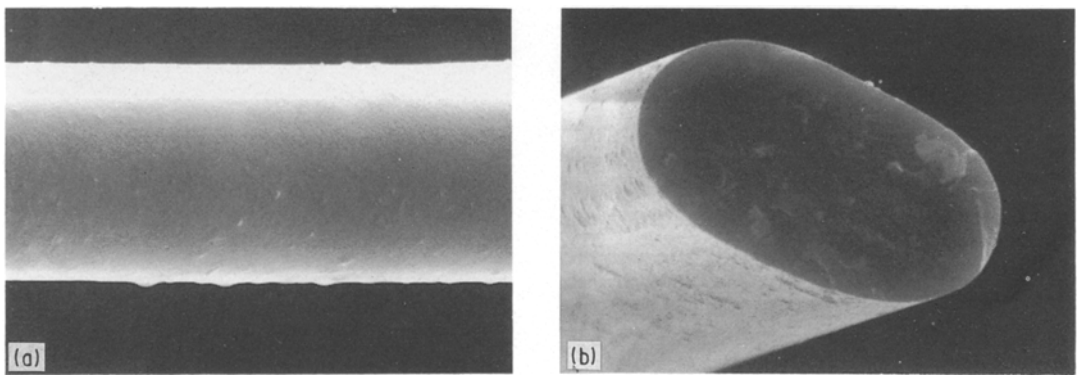

Figure 1 Surface morphology of as-fabricated HPZ fibre.

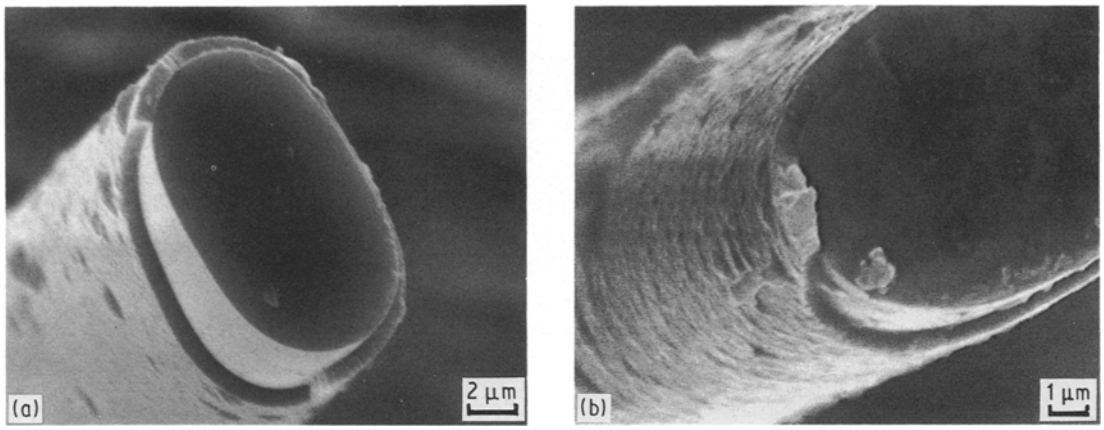

Figure 2 Fracture morphologies of CVI-coated fibres: (a) SiC coating only, (b) pyrolytic C + SiC coating.

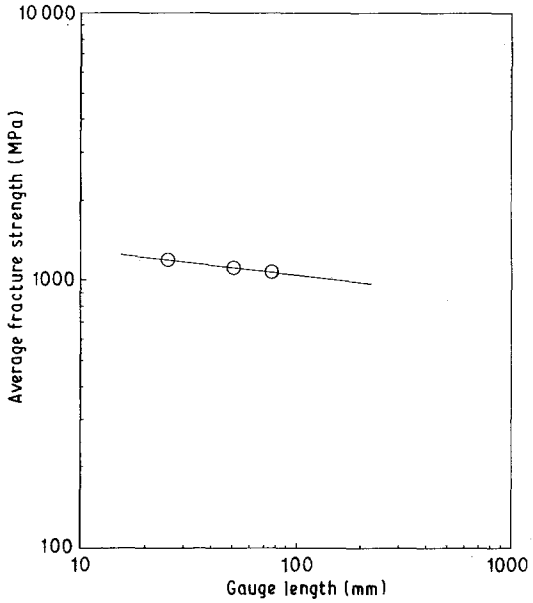

Figure 3 Average tensile strength of as-fabricated fibre as a function of gauge length.

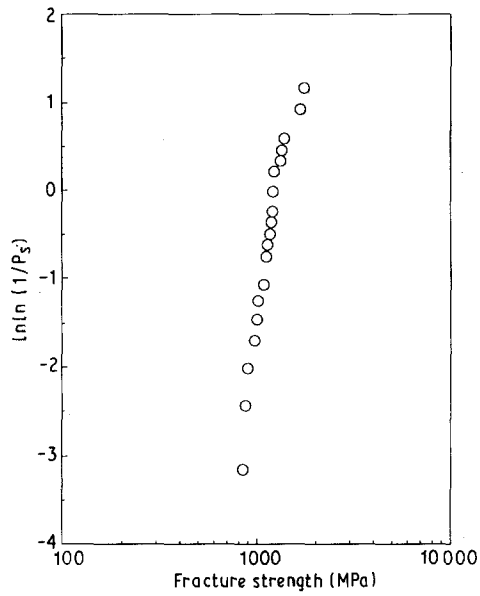

Figure 4 Weibull plot of as-fabricated fibres under tension.

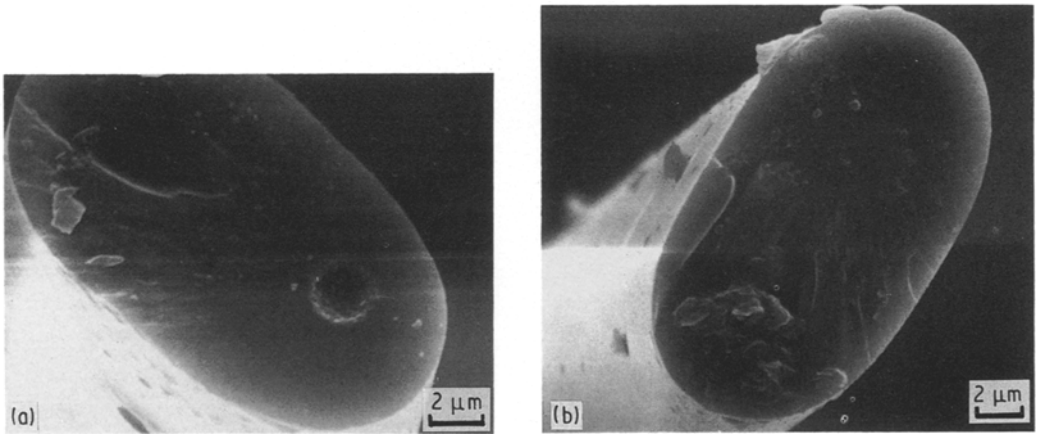

Figure 5 Fracture morphologies of as-fabricated fibres under tension: (a) internal flaw, (b) surface flaw is observed, respectively.

These values are very similar to those of the as-fabricated fibre. However, for the fibres coated with SiC, the average tensile strength drops dramatically to 617 MPa while the Young's modulus increases to 290 GPa. For those coated with pyrolytic C/SiC, the average tensile strength is 830 MPa and the Young's modulus is 197 GPa. The fracture morphologies of the coated fibres are shown in Fig. 2. These fractographs show that fibres with pyrolytic C coating exhibit the same fracture feature as that of the uncoated fibre. That is, fracture is initiated from the surface or internal flaws. Nevertheless, for SiC-coated fibre, the frac-

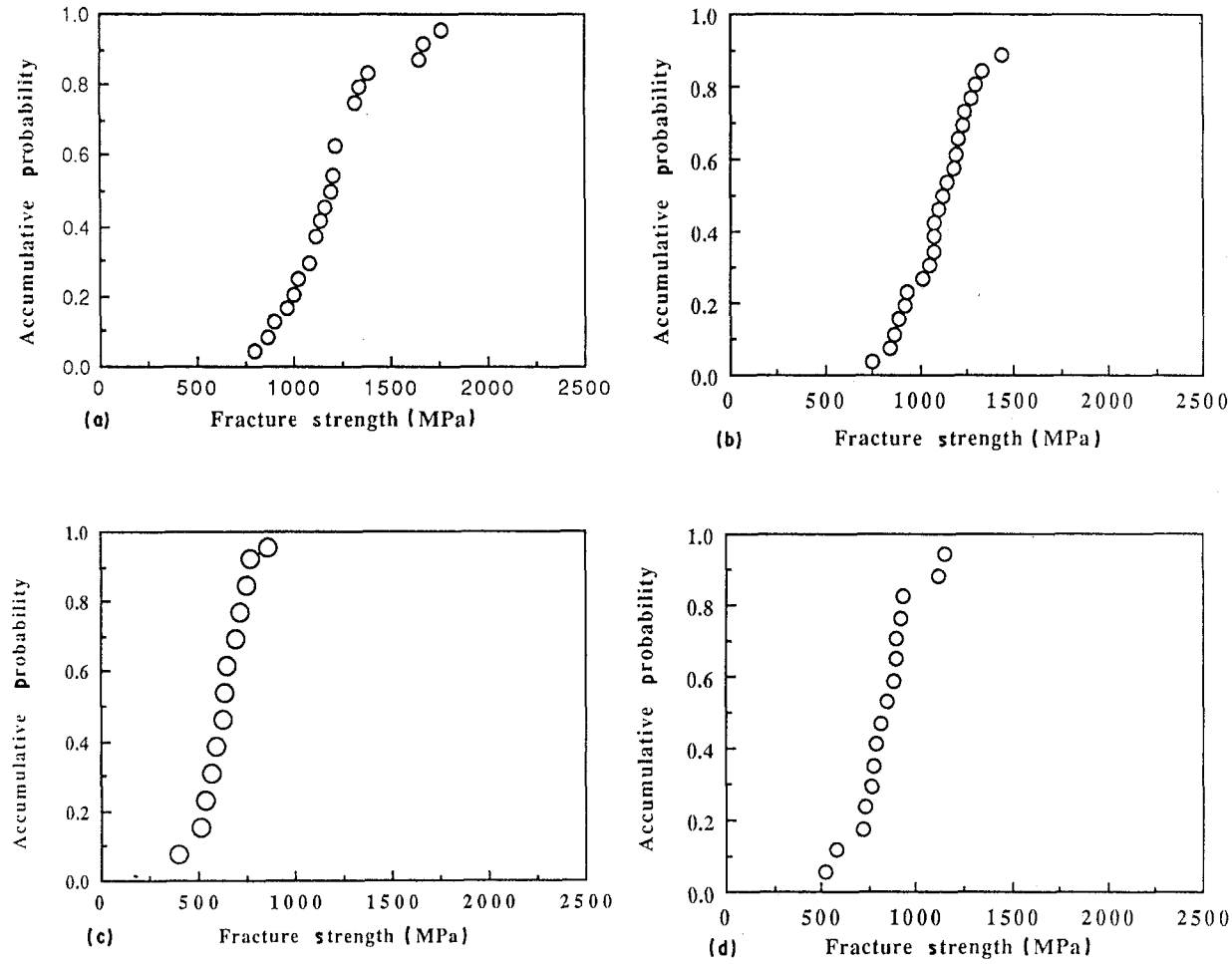

Figure 6 Strength distribution of (a) as-fabricated, (b) with pyrolytic C coating, (c) with SiC coating, (d) with pyrolytic C + SiC coating.

ture morphology is different. Fracture was found to be initiated from the SiC coating layer instead of from the intrinsic/surface defects in the fibre.

3.3. Thermal stability

The results of thermal stability evaluation are illustrated in Figs 7–9. Figs 7 and 8 show the residual tensile strength of the as-fabricated and coated (pyrolytic C/SiC) fibres, respectively, after thermal ageing at 950 °C in vacuum for different periods of time. After 650 h, the as-fabricated fibre retains about 88% of its strength. However, for those fibres coated with pyrolytic C/SiC, the strength remains the same after 260 h. Fig. 9 shows the strength degradation of the as-fabricated fibre at 1200 °C in vacuum. The tensile strength drops to 630 MPa after 66 h in vacuum while the Young's modulus remains the same. For those fibres exposed at 1200 °C in air, strength loss is even more severe. In this case, a thick layer of silica was formed on the fibre surface as shown in Fig. 10. The fracture strength drops to 600 MPa after exposure for only 2 h. Table II summarizes the results of tensile strength, Young's modulus, and Weibull parameter of the HPZ fibres before and after thermal exposure. All of the surface treated and heat-treated fibres exhibited a similar load–displacement curve to that of the as-fabricated fibre.

3.4. Microstructure of the HPZ fibre

Fig. 11 shows the XRD patterns of the HPZ fibre in the as-fabricated state and after thermal exposure at 1200 °C in vacuum for 66 h, respectively. The results show that there is no detectable crystalline phase in the as-fabricated fibre. Also, the diffraction pattern was unchanged after thermal exposure at 1200 °C for 66 h.

4. Discussion

4.1. Strength limiting factors of the ceramic fibre

The most thermodynamically stable phases in the Si–N–C–O system are SiO_2, Si_3N_4, and SiC [6, 7]. However, a previous study shows that HPZ fibre is amorphous and silicon atoms are bonded simultaneously to C, N_2 and O_2 [3]. Because Young's modulus is the macroscopic behaviour of atomic bonding, this non-regularity of bonding might correspond to a wide distribution of Young's modulus as shown in Fig. 12. During the pyrolysis process, a significant weight loss (25–30%) and an increase in density from about 1.0–2.5 $g\,cm^{-3}$ occurs, leading to a large volume shrinkage. Surface and internal defects due to the evolution of a volatile compound would be generated. The results obtained from the tensile test and fracture analysis indicate that the fracture of the fibre is controlled by these local defects.

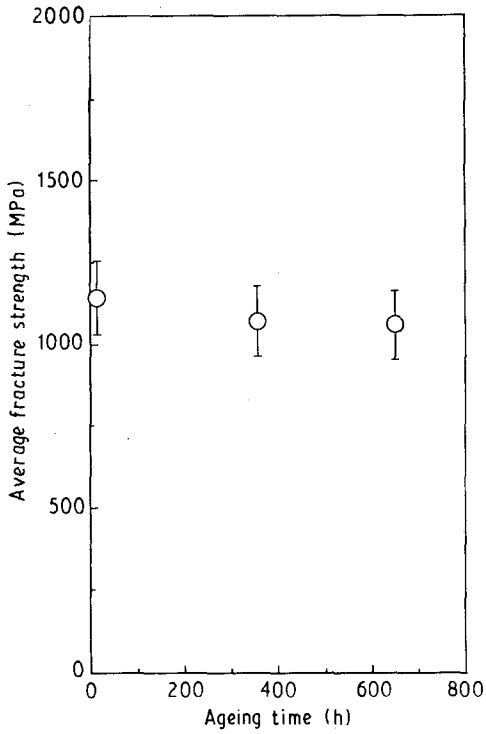

Figure 7 Plot of residual tensile strength of the as-fabricated fibres as a function of thermal exposure time at 950 °C in vacuum.

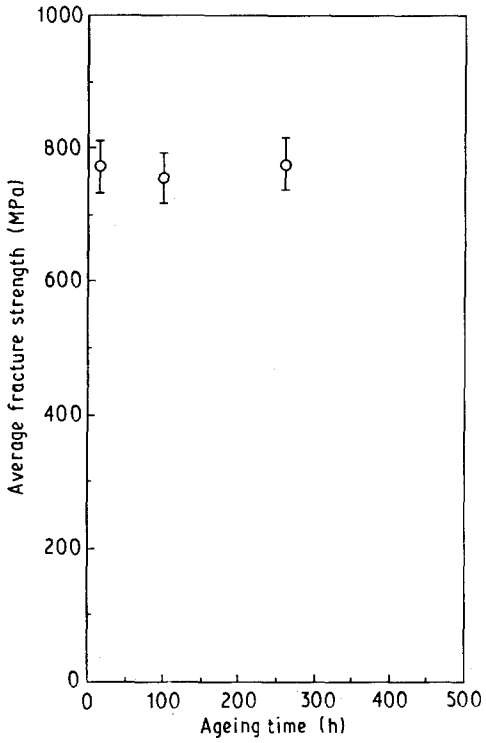

Figure 8 Plot of residual tensile strength of the fibres coated with pyrolytic C + SiC as a function of thermal exposure time at 950 °C in vacuum.

It is well known that, if the defects are of the same type which differ only in size and are spread randomly over the fibre length, the failure obeys the Weibull distribution. The Weibull analysis describes the probability of survival, P_s, of the specimen at a given stress, σ, as a function of its effective volume, V, is given as

$$P_s = \exp\left[- V\left(\frac{\sigma - \sigma_u}{\sigma_o}\right)^m \right] \quad (1)$$

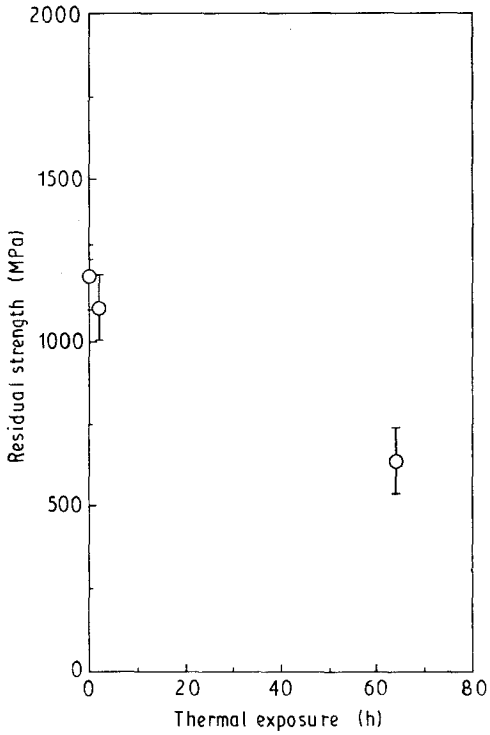

Figure 9 Plot of residual tensile strength of as-fabricated fibres as a function of thermal exposure time at 1200 °C in vacuum.

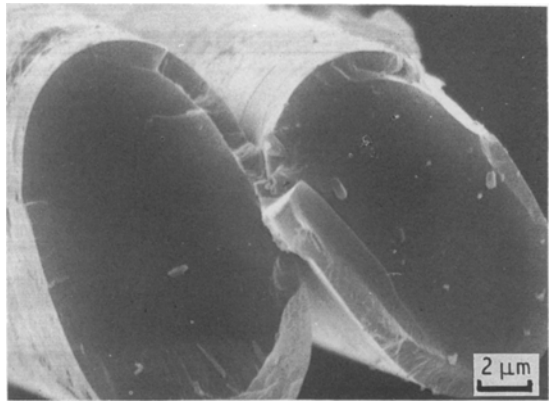

Figure 10 Fracture morphology of as-fabricated fibre thermally exposed at 1200 °C in air for 2 h.

TABLE II Mechanical properties of as-fabricated and treated HPZ fibres

Specimen	Strength (MPa) (average)	Young's modulus (GPa)	Weibull modulus m
A	1196	188 ± 47	5.1 ± 0.3
B	1079	180 ± 23	4.9 ± 0.1
C	632	298 ± 25	4.7 ± 0.3
D	831	197 ± 43	5.1 ± 0.3
A-1	1113	179 ± 56	5.1 ± 0.2
A-2	936	170 ± 46	4.6 ± 0.2
A-3	1054	174 ± 25	5.6 ± 0.4
A-4	1013	188 ± 32	4.8 ± 0.2
D-1	767	188 ± 25	3.8 ± 0.2
D-2	719	188 ± 32	4.2 ± 0.2
D-3	745	187 ± 26	4.2 ± 0.1
A-5	1123	193 ± 39	4.2 ± 0.1
A-6	567	173 ± 15	3.9 ± 0.2
A-8	1120	176 ± 20	4.7 ± 0.2
A-9	581	174 ± 20	4.2 ± 0.3

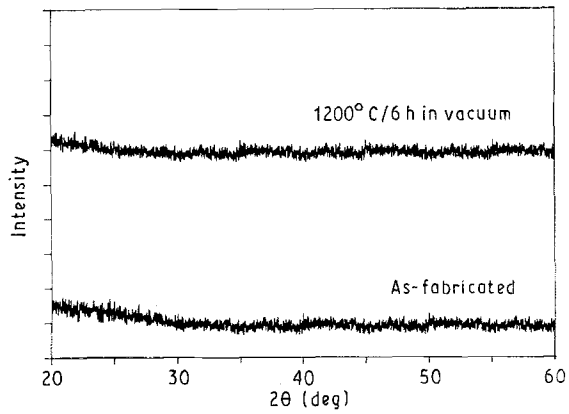

Figure 11 XRD patterns of HPZ fibres, as-fabricated and after thermal exposure at 1200 °C in vacuum for 66 h.

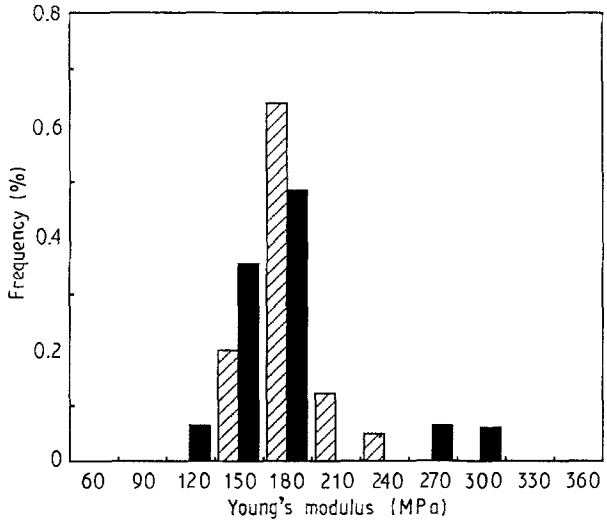

Figure 12 Histogram of Young's modulus of fibres in (▨) as-fabricated state and (■) after thermal exposure at 950 °C for 360 h.

where σ_u is the threshold stress and is usually considered to be zero for ceramics, σ_0 is a constant for the materials, and m is the Weibull shape parameter which characterizes the dispersion of the fracture stress.

Equation 1 can be rewritten as

$$\ln\ln(1/P_s) = \ln(V) + m\ln(\sigma) - m\ln(\sigma_0) \quad (2)$$

Assuming that the fibre diameter is the same, the median stress which corresponds to a 50% failure probability ($P_s = 0.5$) can be written as a function of the fibre gauge length

$$\ln(\sigma_{50}) = -(1/m)\ln(1) + \text{constant} \quad (3)$$

Therefore, it is possible to determine the Weibull shape parameter from either a series of tests using fibres with the same gauge length or by conducting tests on fibres of different gauge lengths. The first approach gives information on the type of defect in material and in particular whether there is a bi- or multimodal distribution of defects which would be shown by a change in gradient. The plot of $\ln\ln(1/P_s)$ as a function of $\ln\sigma$ shows a fairly straight line for the fibres in the as-fabricated state and heat-treated below 1000 °C in vacuum (Fig. 6). This indicates that only one kind of defect population exists in those fibres. Equation 2 also indicates that the Weibull plot of $\ln\ln(1/P_s)$ versus $\ln\sigma$ should result in parallel straight lines for different gauge lengths. For the as-fabricated fibres, the Weibull moduli, m, were determined as 5.1 ± 0.3, 4.6 ± 0.2, and 4.0 ± 0.6 for gauge lengths of 25.4, 50.8, and 76.2 mm, respectively. It is not surprising that the Weibull modulus will be lower for longer gauge lengths due to the possible damage from the handling and testing [8]. Thus, these three Weibull parameters might be considered to be the same.

The second approach allows the median stress value to be determined for any gauge length. The Weibull shape parameter calculated in this way is 9.1 for as-fabricated fibres which is about twice the value determined from constant gauge length. Simon and Bunsell [9] and Anderson and Warren [10] have also reported the same result for Nicalon fibres. However, no explanation has been proposed. Because Weibull statistics have been used successfully to describe the strength distribution of brittle ceramic fibres with constant gauge length, the only possible explanation for this difference is that the relationship between the probability of survival and volume is not in the form of $\exp(-V)$. Assuming that their relationship is $\exp(-V^a)$ in Equation 2 and using the least squares fit, $a = 0.5$ and $m = 4.6$ are obtained. In this case, the Weibull shape parameter calculated by the second approach agrees well with that from the first approach.

For those fibres coated with SiC only, the average tensile strength drops dramatically to 617 MPa while the Young's modulus increases to 290 GPa. The increase of Young's modulus shows that SiC coating (typical value of Young's modulus for CVD processed SiC is about 450 GPa) has contributed significantly to the overall fibre modulus. Also, no internal flaws or mirror–hackle regions were observed on the fibre fracture surface. In other words, strength and failure of this fibre are controlled by surface defects of the brittle SiC coating. This also indicates that the bonding between the fibre and SiC coating is very strong. A brittle fracture with little fibre pull-out would be expected for the uncoated HPZ fibre-reinforced SiC composites. For those fibres coated with pyrolytic C/SiC, the average tensile strength is 830 MPa and Young's modulus is 197 GPa. The increase of tensile strength clearly indicates that pyrolytic C is capable of modifying the bonding between the fibre and the SiC coating (matrix).

4.2. Mechanisms of thermal degradation

As far as the microstructure is concerned, XRD patterns show that HPZ fibre remains totally amorphous after 1200 °C/66 h. This suggests that recrystallization and/or grain growth are not responsible for the degradation of this fibre. However, ceramics in Si–C–O or Si–N–C–O systems are known to degrade in an inert atmosphere at elevated temperatures [10–12]. Above 1000 °C, evolution of N_2 as well as CO and SiO is thermodynamically favourable. In this study, the average tensile strength remains about 88% as-received strength after 950 °C/650 h in vacuum. For those

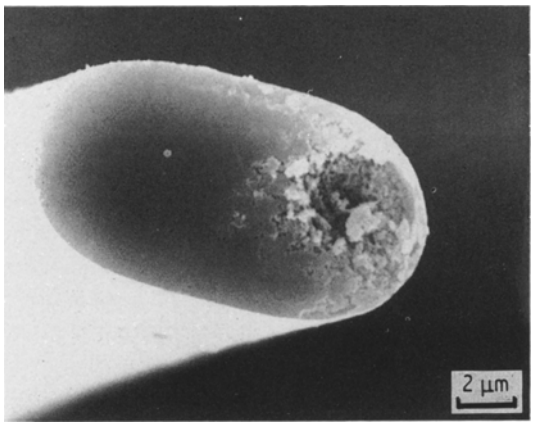

Figure 13 Fracture morphology of uncoated fibre exposed at 1200 °C in vacuum for 66 h.

coated with pyrolytic C plus SiC, the average tensile strength remains the same after 950 °C/260 h. The retention of tensile strength reveals that the pyrolytic C/SiC coating might suppress the evolution of gaseous species.

When thermally exposed at 1200 °C, the average tensile strength drops significantly from 1200–636 MPa after 66 h in vacuum. This may be due to the evolution of gaseous species which leads to larger critical flaws as shown in Fig. 13. For those fibres aged at 1200 °C/2 h, change in strength is negligible. The result suggests that there is kinetic barrier for the decomposition of amorphous Si–N–C–O. Further study on the mechanisms of fibre degradation is needed and is in progress.

5. Conclusions

1. As-fabricated HPZ fibre has an average tensile strength of 1200 MPa, Young's modulus of 180 GPa, and Weibull parameter of 5.1 ± 0.3. Fracture is controlled by the surface and internal flaws. When thermally exposed below 1000 °C, the fibre degradation is negligible. Above 1000 °C, degradation of the HPZ fibre occurs. The fibre degradation might be due to the evolution of CO, SiO, and other gaseous species.

2. Under a typical CVI processing of silicon carbide matrix composite (950 °C and low pressure), the fibre degradation is negligible. Pyrolytic C is needed to tailor the interfacial bond strength between the HPZ fibre and SiC matrix.

3. The microstructure of the HPZ fibre remains amorphous after thermal exposure at 1200 °C/66 h in vacuum. Crystallization and grain growth are not responsible for the thermal degradation of the HPZ fibre at temperatures below 1200 °C.

Acknowledgement

This work was supported by the National Science Foundation (MSM-8809790).

References

1. E. FITZER, in "Whisker- and Fiber-Toughened Ceramics", edited by R. A. Bradley, D. E. Clark, D. L. Larsen and J. O. Stiegler (ASM International, Materials Park, Ohio, 1988) pp. 9–53.
2. T-I. MAH and M. G. MENDIRATTA, *Ceram. Bull.* **66** (1987) 356.
3. Y.-M. CHIANG, J. S. HAGGERTY, R. P. MESSNER and C. DEMETRY, *ibid.* **68** (1989) 420.
4. G. E. LEGROW, THOMAS F. LIM, J. LIPOWITZ and R. S. REAOCH, *ibid.* **66** (1987) 363.
5. C. T. LI and N. R. LANGLEY, *J. Amer. Ceram. Soc.* **68** (1985) C-202.
6. J. A. DICARLO, *J. Metals* **37**(6) (1985) 44.
7. L. C. SAWYER, M. JAMIESON, D. BRIKOWSKI, M. I. HAIDER and R. T. CHEN, *J. Amer. Ceram. Soc.* **70** (1987) 798.
8. S. B. BATDORF and G. SINES, *ibid.* **63** (1980) 214.
9. G. SIMON and A. R. BUNSELL, *J.Mater. Sci.* **19** (1984) 3649.
10. C. H. ANDERSON, R. WARREN, in "Advances in Composite Materials"; ICCM3, Vol. 2, edited by A. R. Bunsell, C. Bathias, A. Martrenchar, D. Menhes and G. Verchery (Pergamon, Oxford, 1980) p. 1129.
11. T. MAH, N. HECHT, D. McCULLUM, J. HOENIGMAN, H. KIM, H. LIPSIT and A. KATZ, *J. Mater. Sci.* **19** (1984) 1191.
12. T. J. CLARK, R. M. ARONS and J. B. STAMATOFF, *Ceram. Engng Sci. Proc.* **6** (1985) 576.

Received 11 July
and accepted 19 November 1990